RAPID COMMUNICATIONS

PHYSICAL REVIEW A VOLUME 40, NUMBER 4 AUGUST 15, 1989

Scaling law for the noise-reduced diffusion-limited aggregation

Fernando Moreira, Rosane R. Freire, and C. M. Chaves
Departamento de Física, Pontifícia Universidade Católica do Rio de Janeiro, rua Marques de São Vicente 225, Caixa Postal 38071, 22453 Rio de Janeiro, Rio de Janeiro, Brazil
(Received 5 April 1989)

We argue that the diffusion-limited aggregation grown with a noise-reduction parameter (B) exhibits three different regimes, according to the relative strength of the fluctuations and lattice-induced anisotropy. A scaling law relating these regimes is proposed. In the intermediate regime the fractal dimension is B dependent. The width of the intermediate regime remains practically constant after a critical value B_c of the noise-reduction parameter, indicating that, however small the fluctuations, lattice anisotropy dominates the process only for scales greater than a screening length.

Since the introduction by Witten and Sander[1] of a model for diffusion-limited aggregation (DLA), a great deal of work has been done (see Meakin[2] and references therein). This is probably due to both the experimental relevance of the model and to the conceptual problems raised by it.

In the original work of Witten and Sander,[1] DLA clusters were self-similar, homogeneous, and isotropic fractals with a density-density correlation function showing power-law decay with distance. The corresponding fractal dimension was independent of the lattice structure. The cluster thus shared the behavior of typical clusters in critical phenomena.

Recently, however, larger clusters obtained by improved simulations seem to indicate some deviations from the above picture. There was the suggestion by Meakin and Vicsek[3] that the DLA cluster is not homogeneous and it shows some anisotropy induced by the underlying lattice,[4-6] and that the fractal dimension may also depend on the lattice structure.[7]

In order to reduce the noise in the simulation and thus accelerate the asymptotic behavior, a change in the DLA rules has been proposed so that each perimeter site becomes occupied only after being reached B times by diffusion particles[2,8,9] ($B=1$ corresponds to the ordinary DLA).

Simulations of DLA clusters grown on a square lattice using this noise-reduction technique (NRT) lead to a star-shaped object (see Fig. 1, also see Ref. 2), even for a relatively small number of particles ($N\sim 3\times 10^3$). This behavior characterizes a regime dominated by lattice anisotropy and is expected to occur only in very large clusters grown without the use of the NRT.

Figure 2, from Fig. 5 of Ref. 2, is the starting point of our analysis. It shows the existence of essentially three different regimes. For a small number N of particles (region I) the aggregates are isotropic with a fractal dimension[1] $D_0\simeq 1.67$. As N grows we eventually reach region III of highly anisotropic clusters with fractal dimension[9] $D_\infty\simeq 1.57$. For intermediate values of N there is a transient behavior resulting from the competition of fluctuations and lattice-induced anisotropy. In this region, which decreases as B increases, the fractal dimension D is B dependent. It is mainly this region that we address below. The initial regime (region I of Fig. 2) corresponds to very small clusters and will not be considered further in this work.

For the crossover II $\rightarrow$ III we can define a characteristic length ξ_B such that for cluster sizes $R\gg\xi_B(R\ll\xi_B)$ the fractal dimension is D_∞ [$D_f(B)$].

The cluster anisotropy at intermediate scales is also a consequence of the existence of two different exponents $\nu_\parallel$ and $\nu_\perp$, governing the growth of the length and the thickness of the cluster arms, respectively ($R_\parallel\sim N^{\nu_\parallel}$ and $R_\perp\sim N^{\nu_\perp}$). At larger scales $\nu_\perp=\nu_\parallel\equiv\nu_\infty=1/D_\infty$.

In the intermediate regime, defining an average radius by $R^{D_f}=R_\perp^{D_f-1}R_\parallel$ allows us to relate D_f, $\nu_\parallel$, and $\nu_\perp$: $D_f\equiv 1/\nu=1+(1-\nu_\parallel)/\nu_\perp$ (see also Ref. 10).

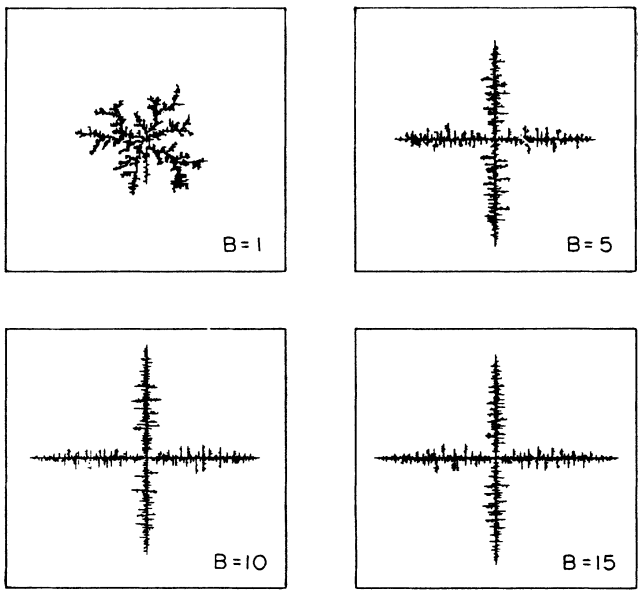

FIG. 1. DLA clusters grown with the noise-reduction parameter $B=1$, 5, 10, and 15 (as indicated). As B increases, the cluster tends to concentrate along the lattice axis. Each cluster has $N=3000$.

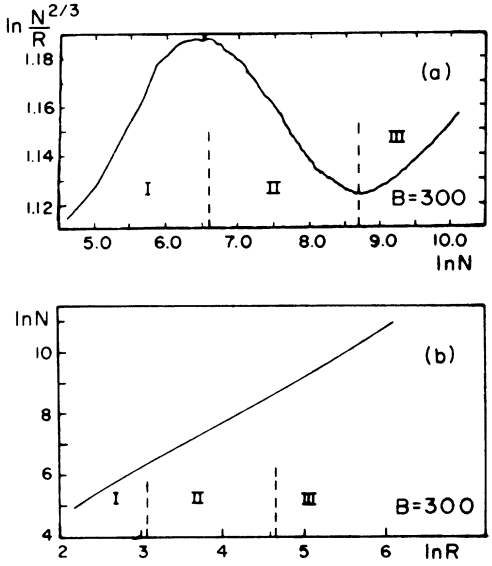

FIG. 2. (a) This plot, which is taken from Fig. 5 of Ref. 2, shows the the existence of three distinct regions during the growth of a DLA cluster. Here $\ln(N^{2/3}/R)$ is plotted against $\ln N$ for $B=300$. (b) Schematic representation of the same data in a plot of $\ln N$ vs $\ln R$. Now the three regions do not show up clearly.

In Fig. 3 we plot $A=\langle\cos 4\theta\rangle$ vs R, for $R<\xi_B$, as a measure of the degree of anisotropy. The principal axis of the lattice have $\theta=n\pi/2$ with n running from 1 to 4, while the diagonal ones have $\theta=(2m+1)\pi/4$, $m=0$ to 3. Thus, the part of the cluster concentrated along the principal axis contributes with 1 to A whereas that part concentrated along the diagonal axis contributes with -1. As a result, for an isotropic cluster we expect $A=0$. An anisotropic aggregate will have $A=\pm 1$ depending on the system of axis along which the cluster tends to concentrate. From Fig. 3 we conclude that the clusters evolve rapidly to an asymmetric shape, though the limiting asymmetry could not yet be achieved for that range of sizes.

From the definitions given above, it follows that

$$A\sim N^{4(\nu_{\parallel}-\nu)}\sim R^{4y}, \tag{1}$$

with $y=(\nu_{\parallel}-\nu)/\nu=(\nu_{\parallel}-\nu_{\perp})(1-\nu_{\parallel})/\nu_{\perp}$. Notice that the knowledge of y and D_f determines the two exponents $\nu_{\parallel}$ and $\nu_{\perp}$.

It is clear from Fig. 3 that the approach to region II is faster as B increases (for $B<B_c$; see below). Coming from region I, where $\nu_{\parallel}=\nu_{\perp}=1/D_0$, this corresponds to an increase (decrease) in the difference $\nu_{\parallel}-\nu_{\perp}(D_f)$. This result is in accord with Meakin.[2] In his plot of $\ln(N^{2/3}/R)$ vs $\ln N$, the slope $(\frac{2}{3}-1/D_f)$ decreases as B increases as region II is reached.

Our plots suggest that after a critical value B_c the width of the transition between the regions remains practically constant. The same is true of the characteristic length ξ_B. We argue below that the very width of the transition region II ($\sim\xi_B$) saturates for $B\geq B_c\sim 20$. Physically this means that the lattice anisotropy, no matter how small the residual fluctuations are, dominates the aggregation process only after a "screening length" ξ_{B_c} for $B>B_c$. Probably ξ_{B_c} and B_c as well are not universal quantities but depend on the lattice.

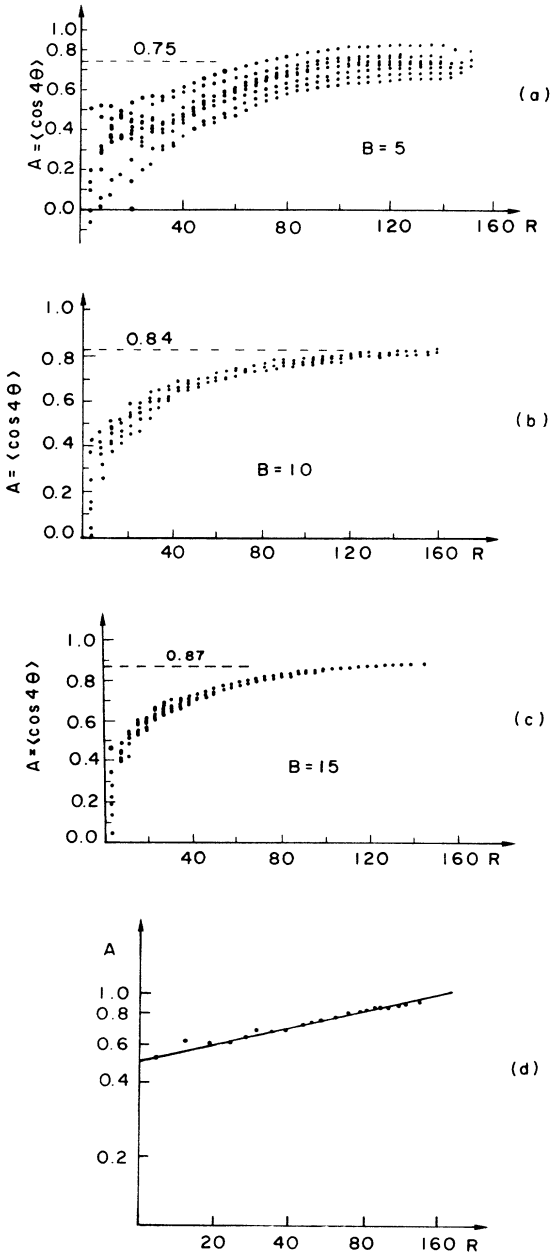

FIG. 3. Plot of the average over the cluster of $\cos 4\theta$ vs the cluster size R for $R<\xi_B$ as a measure of the lattice anisotropy. The lattice principal axis has $\theta=\pi/2$, π, $3\pi/2$, and 2π. (a) $B=5$, (b) $B=10$, and (c) $B=15$. The approach to region II is faster as B increases. (d) As predicted by Eq. (1), a plot of $\log_{10}A$ against $\log_{10}R$ gives a straight line. Here $B=15$.

We propose the following scaling law (all lengths are in units of the lattice parameter)

$$N(R,B)\sim\xi_B R^{D}f_B(R/\xi_B), \tag{2}$$

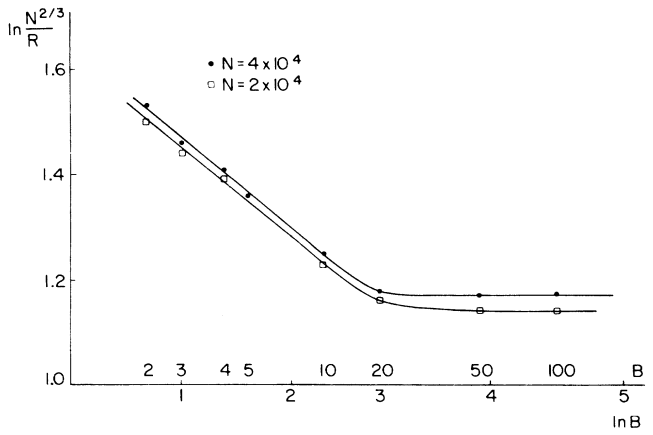

FIG. 4. Plot of $\ln(N^{2/3}/R)$ vs $\ln B$. According to the scaling law (3), for $B < B_c$, a straight line should be obtained, whereas for $B > B_c$, $\ln(N^{2/3}/R)$ tends to a constant. From this plot we estimate $\mu = 0.27$ and $B_c = 16$.

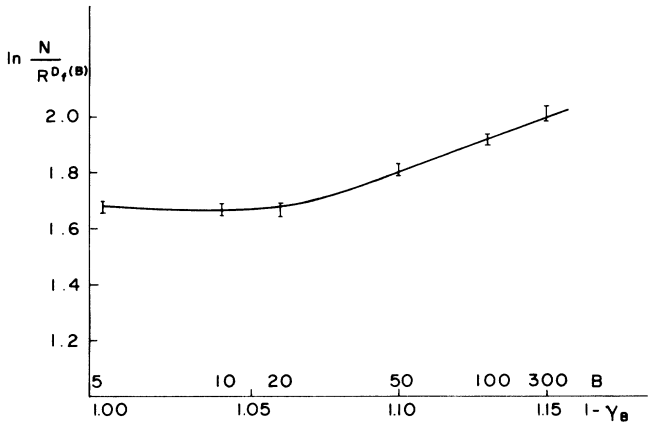

FIG. 6. Plot of $\ln(N/R^{D_f(B)})$ vs $1-\gamma_B$, which, according to (4) is a straight line for $B > B_c$, whose slope is $\ln\xi_B$. Due to the error bars we can only get a rough estimate $\xi_{B_c} = 120$.

where the scaling function $f_B(x)$ is such that

$$f_B(x) \sim \begin{cases} \text{const} & \text{for } x \gg 1, \\ x^{\gamma_B} & \text{for } x \ll 1, \end{cases}$$

introducing an (B dependent) exponent γ_B. As stated above, our data and those of Meakins[2] suggest that ξ_B saturates for large enough B and accordingly we define

$$\xi_B = \begin{cases} \xi_{B_c}, & B > B_c, \\ \xi_{B_c}(B/B_c)^{-\mu}, & B < B_c, \end{cases}$$

thereby introducing a new (B independent) exponent μ.

The scaling law (2) comprises four cases, according to the values of $x = R/\xi_B$ and B/B_c. Typical plots are shown in Figs. 4–6.

In the region $x \gg 1$ our scaling gives

$$N(R,B) \sim \begin{cases} B^{-\mu} R^{D_\infty}, & B < B_c, \\ B_c^{-\mu} R^{D_\infty}, & B > B_c. \end{cases} \tag{3}$$

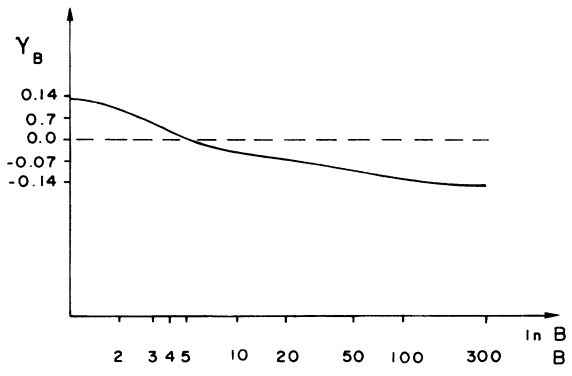

FIG. 5. Plot of $\gamma_B = D_f(B) - D_\infty$ as a function of $\ln B$.

Figure 4 shows the plot of $\ln(N^{2/3}/R)$ vs $\ln B$ (for comparison and use of the data of Ref. 2). For small values of B, the slopes are independent of N (for N large enough) as predicted by (3) and gives $\mu \simeq 0.27$. Between $B = 10$ and $B = 20$ the curves tend to a constant, from which we estimate $B_c^{\mu} \simeq 2.1$, thus giving $B_c \simeq 16$.

For $x \ll 1$ our scaling gives

$$N(R,B) = \begin{cases} \xi_{B_c}^{1-\gamma_B} (B/B_c)^{\mu(\gamma_B - 1)} R^{D_f(B)}, & B < B_c, \\ \xi_{B_c}^{1-\gamma_B} R^{D_f(B)}, & B > B_c, \end{cases} \tag{4}$$

where $D_f(B) = D_\infty + \gamma_B$. From the first relation in (4) we determine $D_f(B)$ and thus γ_B, which is plotted in Fig. 5 (because the transition region is large for small B the error bars—not shown in Fig. 5—are larger for $B \lesssim 5$).

The second relation in (4) predicts that a plot of $\ln(N/R^{D_f(B)})$ vs $(1-\gamma_B)$ would give a straight line whose slope is $\ln\xi_{B_c}$. Figure 6 shows that the data are compatible with this scaling for $B \gtrsim 20$. A fitting allows us to get a rough estimate of the "screening length" $\xi_{B_c} \simeq 120$.

We have proposed a scaling law [Eq. (2)] and verified that our simulations and those of Meakin[2] are compatible with it. One important aspect of this scaling is the prediction of a critical value B_c, beyond which the width of the intermediate region remains practically constant.

The growth of DLA clusters is rather complex. However through the introduction of a scaling law, it seems to be possible to capture the essential steps of the growth process.

This work was supported by the Brazilian Agencies Financiadora de Estudos e Projetos and Conselho Nacional de Desenvolvimento Científico e Tecnológico. We would like to acknowledge useful discussions with Dr. Belita Koiller.

[1]T. A. Witten, Jr. and L. M. Sander, Phys. Rev. Lett. **47**, 1400 (1981); Phys. Rev. B **27**, 5686 (1983).
[2]P. Meakin, Phys. Rev. A **36**, 332 (1987).
[3]P. Meakin and T. Vicsek, Phys. Rev. A **32**, 685 (1985).
[4]P. Garik, Phys. Rev. A **32**, 1275 (1985).
[5]P. Meakin, J. Phys. A **18**, L661 (1985).
[6]R. C. Ball and R. M. Brady, J. Phys. A **18**, L809 (1985).
[7]L. Turkevich and H. Scher, Phys. Rev. Lett. **55**, 1026 (1985).
[8]J. Kertész and T. Vicsek, J. Phys. A **19**, L257 (1986).
[9]P. Meakin, J. Kertész, and T. Vicsek, J. Phys. A **21**, 1271 (1988).
[10]F. Family and H. Hentschel, Faraday Spec. Discuss. Chem. Soc. **83**, 139 (1987).